



ELSEVIER

Journal of Chromatography B, 743 (2000) 357–368

JOURNAL OF
CHROMATOGRAPHY B

www.elsevier.com/locate/chromb

Isoelectric precipitation of soybean protein using carbon dioxide as a volatile acid

Gerard W. Hofland^{a,b,*}, Aris de Rijke^a, Russell Thiering^c, Luuk A.M. van der Wielen^b, Geert-Jan Witkamp^a

^aLaboratory of Process Equipment, Leeghwaterstraat 44, 2628 CA, Delft University of Technology, Delft, The Netherlands

^bKluyver Laboratory of Biotechnology, Julianalaan 67, 2628 BC, Delft University of Technology, Delft, The Netherlands

^cSchool of Chemical Engineering and Industrial Chemistry, University of New South Wales, Sydney, NSW 2052, Australia

Abstract

A novel process is presented for the isoelectric precipitation of soy protein, using carbon dioxide as a volatile acid. By contacting a soy meal extract with pressurized carbon dioxide, the solution pH was decreased to the isoelectric region of the soy proteins. Complete precipitation of the precipitable soy proteins could be achieved for protein concentrations up to 40 g/l at pressures less than 50 bar. Isoelectric precipitation with a volatile acid enabled accurate control of the solution pH by pressure and eliminated the local pH overshoot, usual in conventional precipitation techniques. The advantage of the improved precipitation control was reflected by the morphology of the precipitate particles. Protein aggregates formed by CO₂ were perfectly spherical whereas protein precipitated by sulfuric acid had an irregular morphology. The influence of process variables to control particle size is discussed. © 2000 Elsevier Science B.V. All rights reserved.

Keywords: Isoelectric precipitation; Soy protein; Carbon dioxide

1. Introduction

Industrial processing of proteins is often complex and usually requires auxiliary materials to separate and purify the desired components. Unit operations such as aqueous two-phase partitioning, precipitation and also chromatography require considerable amounts of chemicals to change the pH, ionic strength, or the electric permittivity of a protein medium. Where the produced amounts increase, it is important for environmental reasons to reduce the consumption of the auxiliary compounds in these

process. The auxiliaries are often salts, acids and bases, which cannot be easily recycled.

In recovery of proteins, precipitation remains to be an important technique for concentration and purification. In terms of production volumes, food proteins make up the greater part of the commercially purified protein. Purification of food proteins is in many cases done by means of isoelectric precipitation. Usually, mineral acids such as sulfuric acid and hydrochloric acid are used in these processes. These must be neutralized afterwards, leaving residual salt both in the protein and the residual solution. The use of volatile electrolytes, such as carbon dioxide, can therefore be a valuable tool. After depressurization, the solution returns to a pH close to neutral as the electrolyte returns to the vapor phase.

A second advantage of the use of a volatile

*Corresponding author. Leeghwaterstraat 44, NL-2628 CA, Delft, The Netherlands. Tel.: +31-15-2783-839; fax: +31-15-2786-975.

E-mail address: g.w.hofland@wbmt.tudelft.nl (G.W. Hofland)

electrolyte is that it prevents local overshoot in pH during acidification of the solution. In conventional processes, problems have been reported to occur due to extreme pH values near the acid injection port, which may result in a reduction of precipitate purity and denaturation of the protein [1]. Using a volatile acid, the acid concentration is limited by pressure via the vapor–liquid equilibrium, and hence pH cannot fall below its equilibrium value.

Up to now, the application of carbon dioxide in the isoelectric precipitation has only been investigated for the milk protein casein. The use of carbon dioxide was first described by Jordan et al. [2] using rather simple equipment. Tomasula and co-workers [3,4] further investigated the process both batchwise and continuously and found interesting applications in making improved casein sheets [5]. Gevaudan et al. [6] investigated the effect of CO₂ treatment on the buffering properties of the milk. Hofland et al. [7] compared the carbon dioxide induced casein precipitation with conventional precipitation techniques with respect to yield and mineral partitioning by using high-pressure pH measurements.

Casein is, however, not the only protein produced on a large scale by isoelectric precipitation. The technique is also commonly applied to isolate many plant proteins, among which soy protein is the best known. The precipitation of soy protein isolates differs substantially from the precipitation of casein. It resembles, however, the precipitation of other vegetable proteins and is therefore a widely studied model material. The precipitation of soy protein using mineral acids has been investigated extensively by the groups of Dunnill [8–14] and Glatz [15–21]. Optimization and modeling of the particle characteristics in relation to their centrifugal recovery has been a central theme in these papers.

In this work, the potential of CO₂ as recyclable precipitant in the isoelectric soy protein precipitation is discussed. Important questions as to what pressure is required to reach the isoelectric point and what yield can be achieved, are investigated. A thermodynamic model to describe the behavior of aqueous systems pressurized with CO₂ earlier applied for casein [7] is now adapted for soy protein systems. The yield and particle characteristics are compared to soy precipitates from conventional acid processing at various processing conditions.

2. Theoretical background

2.1. Properties of carbon dioxide as an volatile acid

Conventionally strong acids are used for the isoelectric precipitation of proteins. Carbon dioxide is not a strong acid. Actually, the dissociation constant is quite small (K_a $4.7 \cdot 10^{-7}$ at 25°C). In addition, the solubility of carbon dioxide is low at atmospheric pressures (4.9 mg/kg), as a consequence of which carbon dioxide is usually regarded as a poor acid. On the other hand, it is because of these characteristics that it can be used for mild and reversible acidifications, using the pressure as a process variable.

The pH range for which CO₂ can be used as a volatile acid is indicated in Fig. 1, which shows the various dissociation forms of carbon dioxide (Fig. 1). The lower limit of this range lies at approximately pH 4. Below this value, the fraction of HCO₃⁻ becomes extremely small, indicating that this is about the minimum pH to which carbon dioxide can acidify a solution. At pH values higher than 8.5, the fraction of CO₂ in solution approaches zero, indicating that this is practically the maximum pH for which carbon dioxide is volatile.

Together these roughly mark the pH range. The pH requested for soy protein precipitation lies within this range. Soy proteins isolates are normally produced by precipitation at pH 4.5–5, after aqueous extraction from defatted soy meal or soy flakes at pH

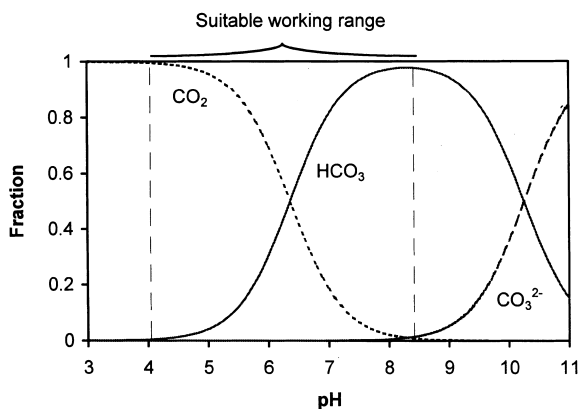


Fig. 1. Fractions of the various ionic forms of CO₂.

ranging between 7 and 10 [22]. Soy meal contains approximately 50% (w/w) protein. Only a part of the soy proteins in soy meal, mainly consisting of glycinin and β -conglycinin, are acid precipitable. Considered as one fraction, the isoelectric point, or better the point of minimum pH, was determined to be pH 4.8 [9], which has been used as endpoint in many precipitation studies.

2.2. Calculation of pH in complex aqueous systems pressurized with carbon dioxide

For engineering purposes it is important to be able to calculate the pressure required to obtain a certain pH in solution, as a function of protein concentration and temperature. In order to do this, the following procedure was followed.

The calculation of the pH in solution requires, firstly, information on the buffering capacity of the components in the liquid phase. Calculating the buffering capacity of the mixture of soy proteins on the basis of the amino acid composition is not very accurate for two reasons. Firstly, pK_a values of amino acids in a protein molecule deviate from that of free amino acids. And secondly, there is some variation in the composition of the soybeans and the degree of extraction of the individual proteins from the soybean. For such systems it is more accurate and simpler to determine the uptake of protons from an experimental titration curve of the solution using a mineral acid, assuming that the type of acid and static pressure do not affect the uptake. In this manner, the uptake of protons by the soluble constituents of the soy meal can be described by an exponential equation:

$$\text{uptake}_{\text{H}^+} = 0.049 + 5.83 \cdot e^{-\text{pH}/1.84} \quad (1)$$

where $\text{uptake}_{\text{H}^+}$ is in mol per kg soy meal.

In addition, the calculation requires the dissociation equilibria and phase equilibria of carbon dioxide and water. This results in the following equations:

$$K_{\text{CO}_2} = \frac{a_{\text{H}^+} \cdot a_{\text{HCO}_3^-}}{a_{\text{CO}_2} \cdot a_{\text{H}_2\text{O}}} \quad (2)$$

$$K_{\text{HCO}_3^-} = \frac{a_{\text{H}^+} \cdot a_{\text{CO}_3^{2-}}}{a_{\text{HCO}_3^-}} \quad (3)$$

$$K_{\text{H}_2\text{O}} = \frac{a_{\text{H}^+} \cdot a_{\text{OH}^-}}{a_{\text{H}_2\text{O}}} \quad (4)$$

where a_i is the activity and K_i the dissociation constant of component i . At 25°C, the dissociation constants in water are 6.36, 10.33 and 14.00, respectively [23]. To account for non-ideality of the liquid phase, the extended Debye–Hückel approximation was used. The set of equations determining the liquid phase concentrations is completed with the electro-neutrality condition:

$$m_{\text{H}^+} + \text{uptake}_{\text{H}^+} - m_{\text{OH}^-} - m_{\text{HCO}_3^-} - 2 \cdot m_{\text{CO}_3^{2-}} = 0 \quad (5)$$

With molal concentration of CO_2 known, the partial pressure can be calculated assuming Henry's law to be valid. The equality of the fugacities of carbon dioxide and water in both phases results in the following set of equations:

$$m_{\text{CO}_2} \gamma_{\text{CO}_2} H_{\text{CO}_2} = \phi_{\text{CO}_2} y_{\text{CO}_2} P \quad (6)$$

$$m_{\text{H}_2\text{O}} \gamma_{\text{H}_2\text{O}} P_{\text{H}_2\text{O}}^{\text{sat}} = \phi_{\text{H}_2\text{O}} y_{\text{H}_2\text{O}} P \quad (7)$$

where H_{CO_2} is the Henry coefficient of CO_2 , $P_{\text{H}_2\text{O}}^{\text{sat}}$ the saturation pressure of water, ϕ_i and y_i the fugacity coefficient and the mole fraction of component i in the gas phase, respectively. In most cases the partial pressure of water is negligible compared with that of carbon dioxide, and Eq. (7) can be disregarded, assuming y_{CO_2} is equal to 1. A correction was made for the non-ideality of the gas phase at high pressure. The fugacity coefficient was estimated by the theory of corresponding states [24]. The values of the Henry coefficient were taken from Edwards et al. [23]. Table 1 shows the values at some relevant temperatures and pressures.

Table 1
Values of the Henry coefficient and fugacity coefficient at some process conditions

	At 5°C, 1 bar	At 5°C, 25 bar	At 25°C, 1 bar	At 25°C, 25 bar
H_{CO_2} (kg bar/mol)	15.44	15.96	29.08	30.01
ϕ_{CO_2} (-)	0.994	0.853	0.995	0.882

This modeling procedure is further detailed in Hofland et al. [7].

3. Experimental

3.1. Precipitation reactor set-up

High-pressure experiments were performed in a 1-l jacketed high-pressure vessel, which was equipped with a magnetically coupled stirrer and two sightglasses (Fig. 2). The inner diameter of the vessel was 84 mm. The impeller was a four-bladed PTFE pitched blade (45°) 46 mm in diameter, mounted at 28 mm from the bottom. The vessel was charged with soybean extract. Carbon dioxide pressure was set by a pressure regulator and its inlet temperature was controlled by a coiled tube heat exchanger. Pressure, temperature, pH and mass of CO_2 transferred to the vessel were measured on-line and recorded on a personal computer.

3.2. Extraction of soy meal

Soy protein solution was prepared according to the standard procedure outlined by Bell and Dunnill [10]. Defatted soy meal (Sigma, S-9633, lot 125H0731, St. Louis, MO, USA) was dispersed in demineralized water to give a final concentration of 10% (w/w). The pH was increased to pH 9.0 by addition of 1 M NaOH whilst stirring for 30 min, taking care to avoid foaming. The dispersion was then centrifuged for 2 h at 4100 rpm. The superna-

tant, the total water extract (TWE) was prepared freshly every day and used within 1 h.

3.3. Determination of pH–pressure profiles

The relationship between pH and pressure was determined for water and soy protein extracts by means of stepwise increasing the pressure and equilibrating after each step. The stirring rate was kept high (800 rpm) to facilitate the mass transfer of carbon dioxide. Equilibration took about 25 min at low pressures and 10 min at high pressures for the pH to become constant. The equilibrium pH was determined at stagnant conditions.

3.4. Precipitation experiments

In order to determine the influence of protein concentration on the precipitation process, experiments were performed with 20, 4 and 0.2 g/l soybean protein solutions. The initial protein concentrations were similar to those in the continuous experiments of Glatz and Fisher [19]. All experiments were performed at a temperature of 25°C and a stirring rate of 300 rpm which corresponded to a power input of 50 mW/kg.

The effect of stirring rate on the precipitation process was determined at agitation rates of 50, 300 and 800 rpm for 20 g/l extract at 25°C and pH 4.8 (pressure of 25 bar). The agitation rates corresponded to power inputs of 0.2, 50 and 980 mW/kg. The experiments were terminated when they reached equilibrium which was defined by a pH value 0.05 units from the expected equilibrium pH at that pressure. As the stirrer speed had a large effect on the uptake rate of carbon dioxide, the process times differed significantly: 50 min, 15 and 3 min, respectively.

For reference, a series of experiments was carried out with sulfuric acid. The process conditions in the experiments, such as protein concentration, stirrer speed and temperature were maintained at 20 g/l, 300 rpm and 25°C , respectively. The addition rate of the sulfuric acid was set in such a way that the total acidification time was the same as in the corresponding experiment with carbon dioxide. The acidification time then amounted to approximately 15 min.

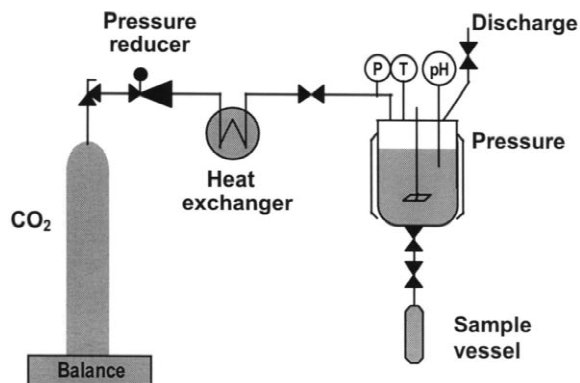


Fig. 2. Experimental set-up used for high-pressure experiments.

3.5. Analytical procedures

Precipitation yield was calculated from the decrease in total protein content in the solution. Slurry samples were withdrawn from the bottom of the precipitation reactor, using a high-pressure sample vessel. The sample was centrifuged for 15 min at 4100 g. The supernatant, or whey, was analyzed for protein concentration using the bicinchoninic acid (BCA) protein assay of Pierce (Rockford, IL, USA). In later experiments, the yield of the precipitation was also determined gravimetrically from the dry mass of the total mass of protein precipitate. Precipitate was dried in an oven at 70°C during 24 h. It was assumed that the dry mass consisted only of protein. Bell and Dunnill [10] found this method to be accurate within 5% of the analyses performed by redissolution of the precipitate and determination of total protein content with the Lowry protein assay.

Particle morphology of the precipitate was characterized by scanning electron microscopy (SEM) (Jeol JSM 5400, Tokyo, Japan). Microscopy samples were prepared by slowly withdrawing a small volume of suspension from the precipitation vessel. A drop (approx. 0.02 g) of the suspension was diluted in 50 ml 1% (w/w) glutaraldehyde solution in order to fixate the precipitate structure [16,18,25]. The diluted suspension was dried under vacuum and sputtered with gold.

Detailed particle size analysis was performed with a Coulter Multisizer II (Luton, UK). It was equipped with a 50 μm or a 280 μm measurement tube and calibration with latex particles of 5.24 μm and 82.3 μm , respectively. Suspension withdrawn from the reactor (ca. 0.02 g) was diluted in 100 ml of 0.07 M sodium acetate buffer (pH 4.8). The buffer solution was filtered before use (0.3 μm , Millipore, Molsheim, France).

4. Results and discussion

4.1. Acidification of soy protein extracts with carbon dioxide

The effect of carbon dioxide pressure on the acidification of soy protein extract solutions was studied as a function of protein concentration and

temperature. Experiments were performed by measuring the equilibrium pH after sequential pressure steps. The experiments were performed for different concentrations of soy protein extract as well as for pure water (Fig. 3). The curves of pH as a function of pressure all have the same pattern. At lower pressures, pH is strongly influenced by pressure increase, and at higher pressures the pH drop is minimal. The protein concentration greatly determines to what extent the pH can be decreased. In case of pure water, a pH of 3.1 can be attained at a pressure of 55 bar. In soy protein solutions of 4, 20 and 40 g/l, the equilibrium pH subsequently increased to 4.05, 4.55 and 4.75 at 55 bar. So, the isoelectric point (pH 4.8) could be reached for each concentration investigated. Of course, the pressure that was required to reach the isoelectric point increased largely with the initial concentration. A 40 g/l solution required a pressure of 46 bar, whereas the twice diluted solution required 24 bar. This limits the protein concentration that can be worked with, since operating at higher pressures than 50 bar will have no advantage in further decreasing the pH. The sensitivity of pH is already low in the pressure range of 30 to 50 bar. The change in pH is only by 0.13 units in case of the 40 g/l solution. As soon as the saturation pressure – 64 bar at 25°C [26] – is reached, the change in pH becomes negligibly small. This can partly be evaded by working at temperatures above the critical point of CO₂ (31°C). But,

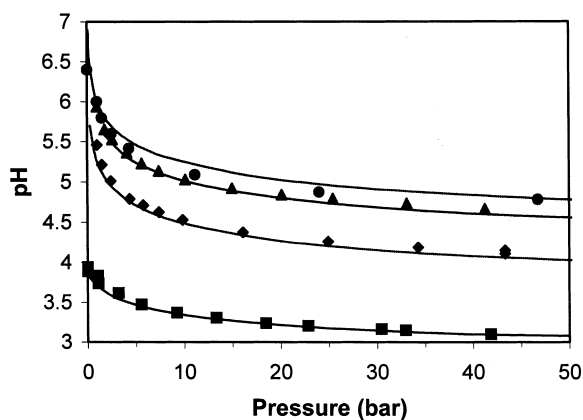


Fig. 3. Measurements (points) as well as calculated values (lines) for pH as a function of CO₂ pressure at 25°C and different soy protein concentrations: ● 40 g/l; ▲ 20 g/l; ◆ 4 g/l; ■ water.

also at supercritical conditions of carbon dioxide, increasing pressure will have only a small effect on pH. It was found by Toews et al. [27] that the pH of water will drop by less than a tenth of a pH unit at carbon dioxide pressures from 80 to 200 bar.

Temperature had little influence on the pH–pressure relationship within the range of 5°C to 25°C for soy protein solutions (Fig. 4). It was expected that the pH would be lower for lower temperatures, due to the higher solubility of CO₂ at lower temperatures. Henry's coefficient for CO₂ is nearly halved from 25°C to 5°C (Table 1), implicating that the solubility is nearly doubled. Temperature however also influences the dissociation constants of the components. The influence of temperature on the dissociation of CO₂ is small in the range 5 to 25°C (Fig. 4) though. Accordingly, the buffering capacity of the protein must have changed with temperature as well.

The acidification of soybean protein solution with carbon dioxide was modeled and is plotted in Fig. 3 as solid lines. The model describes the experimental data reasonably well, both for water and for the protein solutions. Better agreement may be expected when an atmospheric titration curve for each concentration is used. Here, one titration curve was used for all concentrations. Still, some deviations may remain due to inhomogeneities in the material.

The pressure that is required to reach pH 4.80 at 25°C was calculated as function of the soy protein concentration (Fig. 5). The relationship between

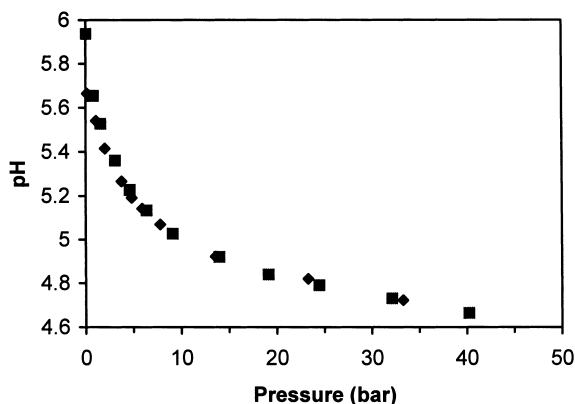


Fig. 4. Influence of temperature on the pH of soy protein extract (20 g/l) as a function of CO₂ pressure at two temperatures: ■ 5°C and ♦ 25°C.

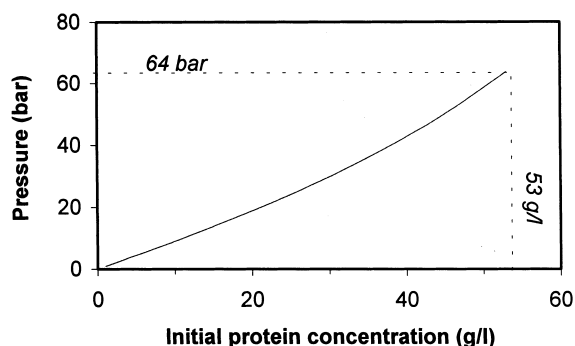


Fig. 5. Calculated pressure required for acidification to pH 4.8 as a function of the initial protein concentration at 25°C. Saturation pressure of CO₂ at 25°C is 64 bar.

pressure and concentration was almost linear. The maximum soy protein concentration that can be acidified to pH 4.80 with gaseous CO₂ was estimated to be 53 g/l at 25°C.

As shown in Figs. 3 and 4, it is possible to control the pH accurately at a certain value in the intermediate pressure range. At low pressure, particularly at sub-atmospheric pressures, the pH is too sensitive to small changes in pressure. At very high pressure, higher than say 40–50 bar, the influence of pressure is so small that disturbances cannot easily be corrected by changing pressure.

4.2. Precipitation yield

Efficient recovery of the product is an important consideration when judging a separation process. High protein recovery increases cost efficiency and reduces waste. To determine the yield, the residual soy protein concentration in the solution was measured as a function of pressure (Fig. 6).

Protein concentration decreases drastically with respect to pressure, to a certain minimum value which reflects the maximum operating pressure required. At these maximum pressures only the whey proteins remain solubilized. If the data are considered in terms of yield and plotted as a function of measured pH (Fig. 7), the maximum yields can be noted to occur at a pH of approximately 4.9, independent of the initial protein concentration. Fig. 7 also shows data points calculated from gravimetric measurement of the solid phase, which give similar

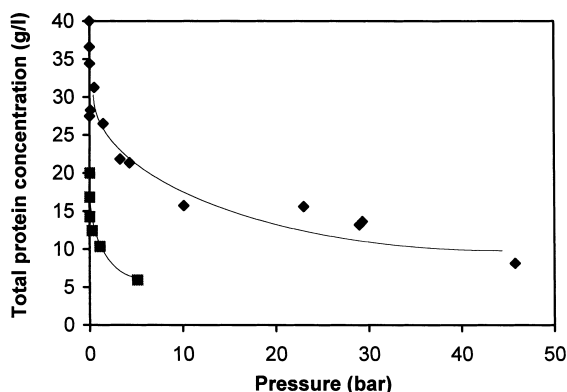


Fig. 6. Residual soy protein concentration as a function of pressure for initial soy protein concentrations of 40 g/l (◆) and 20 g/l (■). Lines to guide the eye.

results. The average yield attained by the batch precipitation of a soybean isolate was $73.6 \pm 4.4\%$ in the range of pH 4.8 and 5.0. Since only a part of the soy protein is acid precipitable, these are very acceptable values. The data are in agreement with data that have been reported for conventional precipitation with mineral acids. Nelson and Glatz [18] established yields of $75.2 \pm 4.6\%$ after precipitation with hydrochloric acid. To exclude errors in the analysis, also reference experiments were performed with sulfuric acid at pH 4.8. The yield of these experiments was found to be $69.7 \pm 3.2\%$, which seems even slightly less efficient, but coincides within the experimental error.

Some authors recommend precipitation at pH values lower than 4.8 [28]. For the CO_2 process,

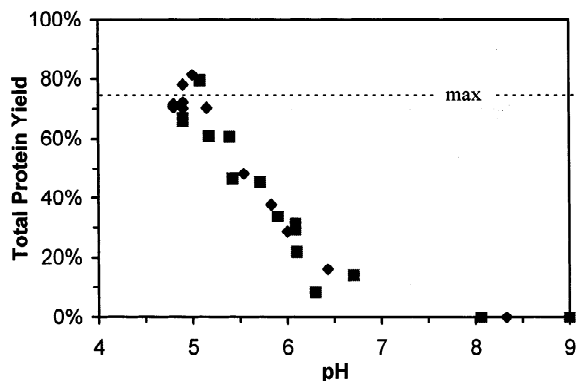


Fig. 7. Precipitation yield of soy protein as a function of pH for initial soy protein concentrations of 40 g/l (◆) and 20 g/l (■).

however, it is preferable to precipitate at the highest pH possible, as this allows the lowest pressures to work at. For an undiluted extract (40 g/l), pH 4.8 requires 46 bar, whereas pH 4.9 and 5.0 need 31 and 22 bar, respectively.

Preliminary work [29] showed that decreasing pressure before centrifugation, did not result in a significant reduction of the yield. Although in industrial processing losses of even less than 0.1% can make a process unprofitable, it may be an option to separate solids at atmospheric pressure, which can be easier and cheaper. An alternative option to centrifugation is the use of filtration membranes. Devereux et al. [30,31] showed that hollow fiber membranes can be used to concentrate soy protein precipitates. A membrane process could be applied under pressure as good as at atmospheric pressure, as long as the pressure difference over the membrane is carefully controlled.

4.3. Particle characteristics

4.3.1. Precipitate morphology from carbon dioxide and sulfuric acid precipitation

The particle characteristics of the precipitate largely determine the ease of recovery of the precipitate. Particle morphology and size of the CO_2 induced precipitation were therefore compared with conventionally prepared soy protein, using a 5% sulfuric acid solution. The process conditions in the experiments, such as protein concentration, stirrer speed and temperature were maintained for both processes at 20 g/l, 300 rpm and 25°C , respectively. Also, the total acidification time was kept constant in both experiments by adjusting the addition rate of the sulfuric acid.

Electron microscopy showed that the shape of the particles differed significantly in the two techniques. Whereas the sulfuric acid induced precipitation (Fig. 9) formed irregularly shaped particles, carbon dioxide formed discrete and regular spheres (Fig. 8). The aggregate size were also larger for volatile electrolyte precipitation. The volumetric mean particle size for carbon dioxide induced precipitation was $34 \mu\text{m}$, while it was only $8 \mu\text{m}$ for sulfuric acid precipitation. The particle sizes resulting from sulfuric acid precipitation agree with those reported by Virkar et al. [9], who found mean particle sizes of

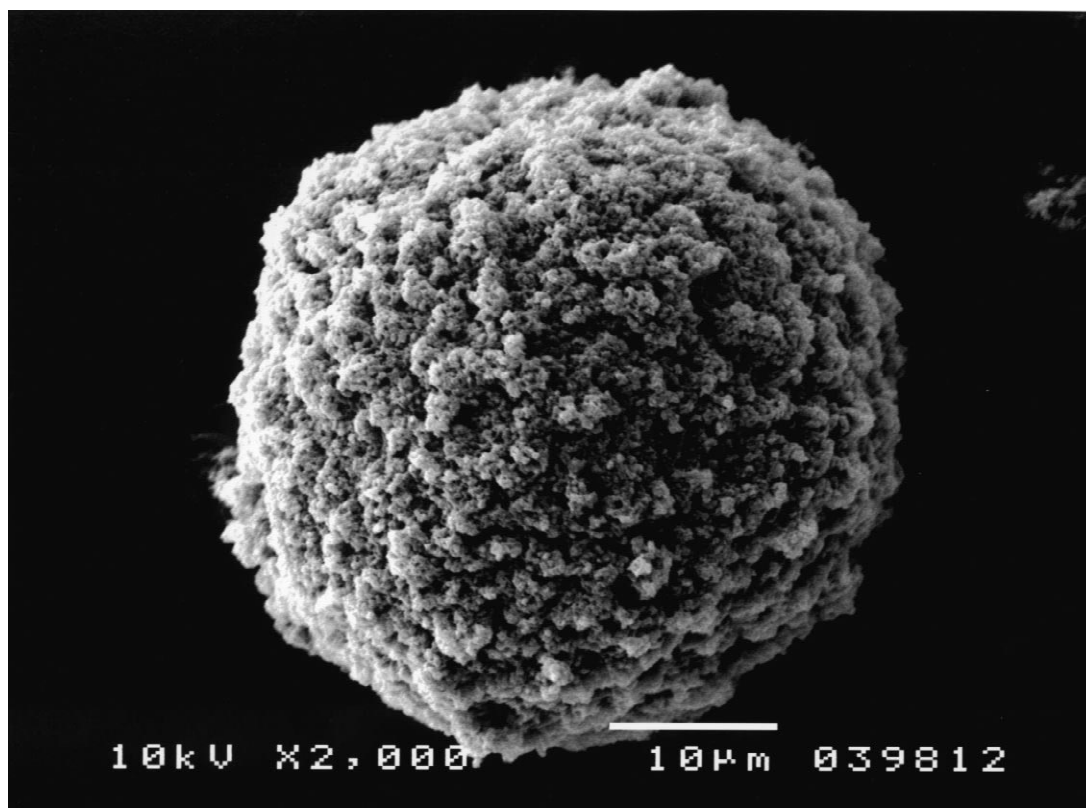


Fig. 8. Typical morphology of aggregates formed using CO₂ as precipitant. Protein concentration 20 g/l, stirring rate 300 rpm, after 30 min.

maximum 9 µm for sulfuric acid precipitation in batch experiments. Hoare et al. [13], however, noted particle sizes ranging between 20 and 30 µm at power inputs between 10 and 50 W/m³, which is more in line with the CO₂ particle sizes found here (at 50 W/m³). The photos in Figs. 8 and 9 further show that the microstructures of the carbon dioxide and mineral acid induced precipitates were similar. That is, both types of particles were aggregates of smaller primary particles of a similar size. This indicates that the type of precipitant influenced the aggregation process, rather than the initial formation and growth mechanism of the primary particles.

The difference in aggregate morphology highlights the importance of precise control over the precipitation process. The intrinsically precise control during carbon dioxide precipitation is due to a number of factors. The first considers the rate of acidification. During the carbon dioxide induced precipi-

tation, the decrease of pH was rapid at first (pH 9–6.5) and then slowed towards the end (pH 5.5–4.8). Specially, in the region of isoelectric point, where aggregation rates are fastest [11], the rate of acidification was slow, resulting in a more controlled aggregate formation.

In addition, there was no local excess of precipitant in the case of carbon dioxide induced precipitation, as occurred at the injection port during sulfuric acid induced precipitation. Using dilute sulfuric acid, the local excess of precipitant could be observed visually by the presence of a completely turbid region (flame) at the injection port by precipitation of protein, already at bulk pH values that were still far above the isoelectric region (pH 7). In the case of CO₂ induced precipitation, at no point in the vessel did the pH fall below its equilibrium pH, as defined by the system pressure. Hence, the pH monotonically decreased with time in each part of

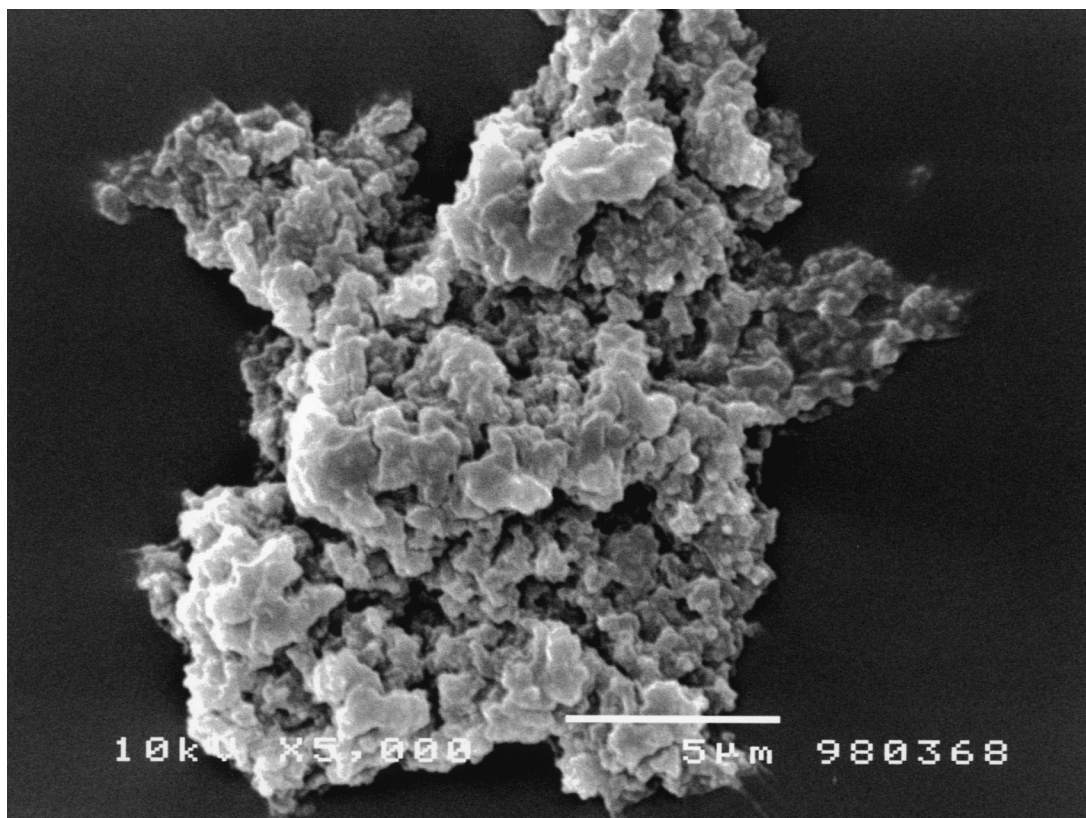


Fig. 9. Typical morphology of the aggregates using sulfuric acid as precipitant. Protein concentration 20 g/l, stirring rate 300 rpm.

the reactor. Consequently, also the solubility will decrease monotonically, which results in a gradually changing supersaturation. The formation of energetically unfavorable particle shapes will then be less probable. In the CO₂ experiments, it was now observed that the turbidity of the solution slowly changed homogeneously over time.

The spherical particles formed with carbon dioxide may have favorable organoleptic properties and are potentially very attractive in some controlled release applications of pharmaceutical components.

4.3.2. Particle size in carbon dioxide induced precipitation

4.3.2.1. Effect of protein concentration. The effect of some process variables were investigated for the carbon dioxide induced precipitation process. Protein

concentration did not influence aggregate shape, only the aggregate size was changed (Fig. 10). It was also noted that the mean diameter of the primary particles was constant: $0.2 \pm 0.03 \mu\text{m}$. This is similar to the

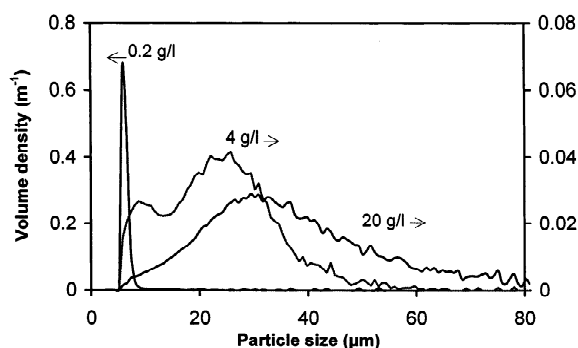


Fig. 10. Influence of initial protein concentration of particle size distribution. Arrows indicate the axis.

results of Nelson and Glatz [18] for precipitation using mineral acids.

The mean aggregate size was found to increase with the initial protein concentration, as expected (Fig. 11). The order of the increase is close to one-third (0.37), which was also found in modeling of the conventional precipitation [20]. The value of one-third originates from the assumption that only the collisions between primary particles and aggregates contribute to the aggregation. Successful collisions between two aggregates are neglected. The rate of aggregate formation is then first order in the primary particle concentration, which rises linearly with the initial protein concentration because the primary particle size remains constant. When the assumption of a constant radial particle density, the volume mean particle diameter will hence be proportional to the initial protein concentration to the power one-third. The results here indicate the same mechanism, although only a few measurements were done.

The increase in particle size means that when a large particle size is desired, a large initial concentration should be applied, even though this requires operating at higher pressures. Increasing pressure will however also result in higher shear when pressure is released after the precipitation, which causes more breakup of particles. It may then well be the pressure release step that determines the particle size rather than the precipitation. This is especially important when solid separation is conducted after pressure release.

For a concentration of 4 g/l, a bimodal distribution was observed. This indicates that breakup

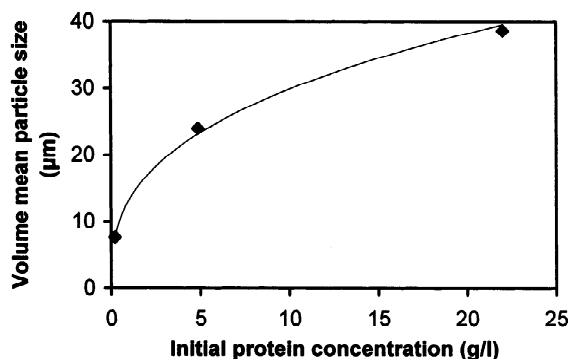


Fig. 11. Volumetric mean particle size as a function of initial protein concentration at 300 rpm.

occurred. In fact, when the mixing time was prolonged bimodal distributions were found for other experiments as well.

4.3.3. Effect of agitation rate

The intensity of mixing had two primary influences on the precipitation mechanism. Firstly, the increase in mixing intensity led to an improvement of the uptake rate of the gaseous precipitant CO_2 into the liquid phase, by an increase of the mass transfer over the vapor–liquid interface as well as an increase of the convective mixing of the precipitant through the liquid phase. This was reflected in an increase in the acidification rate with increasing stirring rate. For stirring rates of 60, 300 and 900 rpm, it needed 50, 15 and 3 min, respectively, to reach the equilibrium pH within 0.05 units. Secondly, stirring directly effected the final particle size by aggregation and breakage of the precipitates.

Despite the differences in acidification times, the volumetric particle size distributions for precipitates, formed across the range of mixing rates, are remarkably similar (Fig. 12). The modes of the distributions are located at similar size. Also the shape of the distributions is alike, except for the extra peak at small diameters for the 800 rpm experiment. This extra peak may be attributed to the increased breakup of aggregates at this high mixing rate. Although not shown in Fig. 12, longer processing times caused the magnitude of this peak to increase at the expense of the larger particles. The distributions for the 50 and 300 rpm experiments showed similar behavior upon aging.

The similarity of the particle size distributions can

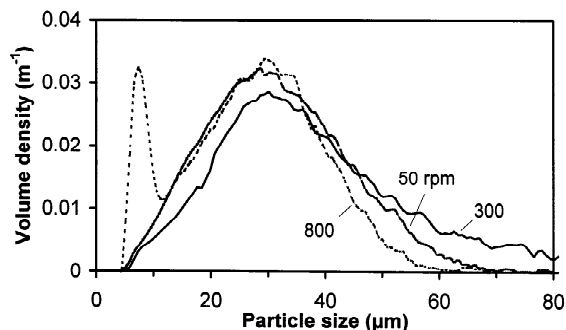


Fig. 12. Volumetric mean particle size as a function of stirring rate at a protein concentration of 20 g/l.

at least partly be understood if the effects of acidification time and hydrodynamic shear are combined. The effect of exposure to hydrodynamic forces is often characterized using the dimensionless Camp number, which is defined as the product of the overall shear rate and the time of exposure. This number has been used to describe breakup during aging [12]. The aggregation rate is often modeled as being linearly dependent in the shear rate, as is breakup [21]. It could therefore also be applied as a measure in the precipitation stage of the process. For the calculation, the time to reach the isoelectric pH is here taken as the exposure time, because during this period of time the solubility is still decreasing. The shear rate was characterized by:

$$\gamma = \sqrt[3]{\frac{P}{V\eta}} \quad (8)$$

where P is the power input (W), V the reactor volume (m^3) and η the dynamic viscosity taken as $1.4 \cdot 10^{-3} \text{ Ns/m}^2$ [9].

Resulting values of the Camp numbers are given in Table 2. It follows from the values that the differences between the experiments are not as large as might be expected from operating conditions themselves. The total exposure to shear is indeed largest for the 800 rpm experiment, which may be interpreted as that the precipitation has progressed the most in this experiment. The values of the 50 rpm and the 300 rpm experiments are close and even switched in position.

The results suggest that it is well possible to operate the acidification stage of the precipitation at higher power inputs without detrimental effects for the particle size, as long as the time of exposure is reduced accordingly. In this way the required residence time can be reduced. As a result, less equipment is required, which is important considering investment costs in high-pressure operations.

Table 2
Values of the Camp number at three stirrer speeds

N (rpm)	Camp number (–)
50	19 000
300	13 000
800	45 000

5. Conclusions

The use of carbon dioxide as a volatile acid has successfully been explored for the precipitation of soy protein. The acidifying properties of carbon dioxide appear to be suitable for effective precipitation of this vegetable protein. The protein concentration largely determines the pressure that is required to reach the isoelectric point (pH 4.8). The yield of precipitation is comparable with sulfuric acid precipitation. The restriction of the precipitant concentration by the phase equilibrium can be used as a tool to locally control minimum pH in the solution. This precise control over pH is believed to be the cause of the formation of spherical aggregates. The particle size is importantly influenced by the initial protein concentration. Decreasing the initial concentration will, therefore, need a lower pressure but also lead to smaller particles. The impact of the power input during the acidification appeared to be small in the performed experiments, probably because also the exposure time changed inversely as the acidification rates changed as well.

Acknowledgements

We gratefully acknowledge Paul Durville for his assistance in the SEM analyses.

References

- [1] D.J. Salt, R.B. Leslie, P.J. Liliford, P. Dunnill, *Eur. J. Appl. Microbiol. Biotechnol.* 14 (1982) 144–148.
- [2] P.J. Jordan, K. Lay, N. Ngan, G.F. Rodley, *NZ J. Dairy Sci. Technol.* 22 (1987) 247–256.
- [3] P.M. Tomasula, J.C. Craig, R.T. Boswell, R.D. Cook, M.J. Kuranz, M. Maxwell, *J. Dairy Sci.* 78 (1995) 506–514.
- [4] P.M. Tomasula, J.C. Craig, R.T. Boswell, *J. Food Eng.* 33 (1997) 405–419.
- [5] P.M. Tomasula, N. Parris, W. Yee, D. Coffin, *J. Agric. Food Chem.* 46 (1998) 4470–4474.
- [6] S. Gevaudan, A. Lagaude, B. Tarodo de La Fuente, J.L. Cuq, *J. Dairy Sci.* 79 (1996) 1713–1721.
- [7] G.W. Hofland, M. Van Es, L.A.M. van der Wielen, G.J. Witkamp, *Ind. Eng. Chem. Res.* 38 (1999) 4919–4927.
- [8] D.J. Bell, D. Heyword-Waddington, M. Hoare, P. Dunnill, *Biotechnol. Bioeng.* 24 (1982) 127–141.

- [9] P.D. Virkar, M. Hoare, M.Y.Y. Chan, P. Dunnill, *Biotechnol. Bioeng.* 24 (1982) 871–887.
- [10] D.J. Bell, P. Dunnill, *Biotechnol. Bioeng.* 24 (1982) 1271–1285.
- [11] M.Y.Y. Chan, D.J. Bell, P. Dunnill, *Biotechnol. Bioeng.* 24 (1982) 1897–1900.
- [12] D.J. Bell, P. Dunnill, *Biotechnol. Bioeng.* 24 (1982) 2319–2336.
- [13] M. Hoare, T.J. Narendranathan, J.R. Flint, D. Heywood-Waddington, D.J. Bell, P. Dunnill, *Ind. Eng. Chem. Fund.* 21 (1982) 402–406.
- [14] D.J. Bell, M. Hoare, P. Dunnill, *Adv. Biochem. Eng. Biotechnol.* 26 (1983) 1–72.
- [15] A.M. Petentate, C.E. Glatz, *Biotechnol. Bioeng.* 25 (1983) 3049–3058.
- [16] G.C. Grabenhauer, C.E. Glatz, *Chem. Eng. Commun.* 12 (1981) 203–219.
- [17] A.M. Petentate, C.E. Glatz, *Biotechnol. Bioeng.* 25 (1983) 3059–3078.
- [18] C.D. Nelson, C.E. Glatz, *Biotechnol. Bioeng.* 27 (1985) 1434–1444.
- [19] C.E. Glatz, R.R. Fisher, *ACS Symp. Ser.* 314 (1986) 109–120.
- [20] C.E. Glatz, M. Hoare, J. Landa-Vertiz, *AIChE J.* 32 (1986) 1196–1204.
- [21] D.L. Brown, C.E. Glatz, *Chem. Eng. Sci.* 42 (1987) 1831–1839.
- [22] K. Liu, in: *Soybeans – Chemistry, Technology and Utilization*, Chapman and Hall, New York, 1997, p. 394.
- [23] T.J. Edwards, G. Maurer, J. Newman, J.M. Prausnitz, *AIChE J.* 24 (1978) 966–976.
- [24] J.M. Smith, H.C. van Ness, *Introduction To Chemical Engineering Thermodynamics*, 4th ed., McGraw-Hill, New York, 1987.
- [25] S. Rohani, M. Chen, *Can. J. Chem. Eng.* 71 (1993) 689–698.
- [26] S. Angus (Ed.), *International Thermodynamic Tables of the Fluid State, Carbon Dioxide*, Vol. 3, Pergamon Press, 1976.
- [27] K.L. Toews, R.M. Shroll, C.M. Wai, *Anal. Chem.* 67 (1995) 4040–4043.
- [28] W.J. Wolf, in: I.A. Wolf (Ed.), *Handbook of Processing and Utilization in Agriculture*, Part 2, Vol 11, CRC Press, Boca Raton, FL, 1983, pp. 23–55.
- [29] G.W. Hofland, A. de Rijke, L.A.M. van der Wielen, G.J. Witkamp, in: *Proceedings of the 14th International Symposium on Industrial Crystallization*, Cambridge, 1999.
- [30] N. Devereux, M. Hoare, P. Dunnill, *Biochem. Biotechnol.* 23 (1986) 422–431.
- [31] N. Devereux, M. Hoare, P. Dunnill, *Chem. Eng. Commun.* 45 (1986) 255–276.